Chapter 4.2 Models projections of ocean warming under “business as usual” and “moderate mitigation” scenarios

Lead Authors:

Bruno Combal and Albert Fischer, Intergovernmental Oceanographic Commission of UNESCO, Paris, France.

Chapter Citation:

Combal, B., Fischer, A. (2016). Chapter 4.2: Model projections of ocean warming under "business as usual" and "moderate mitigation" scenarios. In UNESCO IOC and UNEP (2016). The Open Ocean: Status and Trends. United Nations Environment Programme, Nairobi, pp. 70-89.

4.2 Models projections of ocean warming under "business as usual" and "moderate mitigation" scenarios

4.2.1 Summary and Key Messages

As introduced in Chapter 4.1, the ocean is a key part of the climate system, through its role in the cycles for energy/heat, water, and carbon. Human-induced changes in climate affect the physics of the ocean, which influences marine ecosystems. The Conceptual Framework (Chapter 2) upon which the Open Ocean Component is built, assumes that a policy should target the improvement of human wellbeing. As there is a circular relation between human actions framed by the policies, and the impact of changes of marine services on human society, a scenario accounting for climate mitigation is required to project the current state of the ocean to the future. The IPCC considers 4 possible scenarios in its 5th Assessment (Chapter 4.1 and Glossary Box 2), starting with no change to the current situation and 3 scenarios showing increasingly stringent global mitigation policies.

This Chapter identifies some key indicators of the state of the ocean climate and their projected changes under the IPCC scenarios. Other Chapters in this Report have used these indicators as inputs to models for marine ecosystem response or cumulative human impact. Two of the four IPCC scenarios frame the possible evolution of the ocean: the one corresponding to the progression of radiative forcing without implementing a significant greenhouse gas reduction policy (RCP 8.5) and a best-case scenario with a feasible reduction policy (RCP 4.5). For sake of clarity, scenario RCP 8.5 is referred as "Business As Usual" (BAU), and RCP 4.5 is referred as "Moderate Mitigation" (MM).

A fundamental quantity in determining the role of the ocean in climate and in marine ecosystems is Sea Surface Temperature (SST). It affects the large-scale circulation of the atmosphere, and therefore patterns of rainfall and drought. Since many marine ecosystems are pelagic (near-surface), it is an important input to ecosystem models and estimates of their future state. The combination of a warming and acidifying ocean (see Chapter 4.5) directly threatens species as diverse as coral reefs (see Chapter 5.4) and pteropods (see Chapter 5.5). Climate models project a growth in the tropical warm pool (the area of permanently high temperature, typically above 28°C), the major driver of large-scale tropical atmospheric circulation and surface rainfall and evaporation patterns. Both scenarios show an increase of temperature, especially in Northern Hemisphere high latitudes. They also both indicate that a large fraction of the ocean will experience yearly recurring temperature increases of 2°C or more above the temperature observed in the period 1970-2000.

In Polar Regions, the so far pristine waters house fragile ecosystems. Sea ice creates an important habitat, and is a barrier to human activities: Arctic seas are impassable in winter. In the perspective of the Conceptual Framework driving this assessment (Chapter 2), the future of the Arctic region is found to be more pressing than the Antarctic. The Arctic region actually lacks the comprehensive legal framework that is protecting the Antarctic (Lennon, 2008). This leaves the region vulnerable to human pressures applied by the nearby populations living on its perimeter. The seasonal recession of sea ice is a spatial indicator of seasonal warming. This Chapter shows that in addition to seasonal variation, the total extent of Arctic sea ice has been regressing over the past 30 years. Climate model projections also show that the loss of sea ice in the Arctic is *likely* to be much more significant than in the Antarctic, with impact on navigation, opening access to natural resources and potentially increasing human pressures there. The combination of a lack of governing policies to protect the environment, with intense human pressure and dependence on the ecosystem services drives a concern for the future health of the Arctic ecosystems, and hence a focus of this Chapter.

Global warming has already led to a decrease of the area of Arctic sea ice observed at the end of Northern Hemisphere summers, which in turn may have implications on the global energy balance. With less ice cap surface, less energy is scattered back to space, resulting in more energy absorbed by the Earth's climate system, which in feedback, increases global warming.

This Chapter shows how models outputs are used to get a projection of the ocean variable states to 2030 and 2050. As projections of ocean warming are extensively used in other chapters, details of processing are described here.

In particular, some indicators based on projections of Sea Surface Temperature were computed specifically for this assessment, and they are reviewed in this Chapter. This Chapter also reviews projections and observations of the Polar Sea Ice area change; most of the conclusion being extracted from IPCC Assessment Report 5. Both ocean surface temperature and polar sea ice projection are addressed for BAU and MM scenarios.

Key messages

- The surface ocean is expected to warm, in an ocean-average sense, whether there is mitigation or emissions remain the same;
- Much of the surface open ocean will warm on the order of 1°C, though some will warm 2°C or more (especially in the Northern Hemisphere), under a "Business As Usual" emission scenario, by 2050. Even with mitigation efforts there will be significant surface warming;
- The area of regions with very warm water (>28°C) will increase substantially by 2050 under "Business As Usual" scenario, with *likely* effects on at least regional weather;
- Monthly departures from climatology will be enough to provide substantial thermal stress on many coral by 2050 under "Business As Usual" scenario;
- Arctic summer sea ice extent is expected to continue to diminish, particularly under "Business As Usual" scenario. By 2050 there may be no sea ice at the end of summer.

4.2.2 Main Findings, Discussion and Conclusions

As established in the IPCC's Fifth Assessment Report (IPCC AR5, 2014), Earth global warming affects the ocean thermodynamics and chemistry. Ocean warming dominates the global energy change inventory. Warming of the ocean accounts for about 93 per cent of the increase in the Earth's energy inventory between 1971 and 2010 (*high confidence*), with warming of the upper (0 to 700 metres) ocean accounting for about 64 per cent of the total. The scientific community used climate model simulations for a time-projection of the possible future state of the ocean. As explained in Chapter 4.1, CMIP5 model projections are using four different scenarios, named Representative Concentration Pathways (RCPs), depicting possible future global radiative forcing pathways, because of the adoption of hypothetical mitigation policies (See Glossary Box 2). The groups of researchers run their models for each scenario, resulting in an ensemble of projections. With each model having specific qualities, the ensemble mean of the model projections are considered. The spread of the model ensemble was also considered for an estimate of the disagreement between the models, showing the lowest and highest ranges for a given variable. When all models show similar pattern or trends, the confidence in the projection was enforced.

Different hypotheses of carbon emission regulations determine the four CMIP5 scenarios, corresponding to the various capacities of human society to implement regulations to reduce emissions and in turn lower the final radiative forcing applied to the global climate system. Scenario RCP 8.5 corresponds to the case where no specific policy is applied, often known as the "Business As Usual" scenario, and by such constitutes a base case for future assessment, in the sense that no mitigation policy is applied. To frame the future evolution of the ocean ecosystem, the simplest approach considered that it would be in between RCP 8.5 and a scenario applying reduction policies. The RCP 2.6 seems difficult to reach in practice, therefore RCP 4.5 was the best-case scenario for the work. Because RCP 8.5 corresponds to a direct projection of the present situation, more attention was payed to this scenario. For sake of clarity, scenario RCP 8.5 is referred as "Business As Usual" (BAU), and RCP 4.5 is referred as "Moderate Mitigation" (MM).

This Chapter introduces the analysis of the impact of climate change on the environment, including the biodiversity and human activities. Simple computations show the potential change of the Sea Surface Temperature (SST), computed as the ensemble mean of climate model outputs. The processed data set is available to the reader from the onesharedocean.org platform[23]. The results show how a warming ocean can lead to the expansion of the Indo-Pacific Warm Pool. The same data set was also used for a time projection of the Ocean Health Index (Chapter 8.2).

23 See page http://onesharedocean.org/open_ocean/climate/physical_effects

A simple indicator assessing the potential thermal stress on living organisms was defined. The assessments of stress on coral reefs and pteropods are in Chapters 5.4 and 5.5, respectively. The data generated for this first level of analysis is available to the reader from the onesharedocean.org platform[1]. The impact of global warming on the Arctic sea ice and the potential future state of the Arctic was also described, using observation data and modelling analyses.

All processing codes used in this Chapter are available (under GNU general public license) from https://github.com/IOC-CODE.

Ensemble means of SST projections

One of the most important and direct effects expected from climate change is an increase, at global scale, of the atmosphere and ocean temperatures, which are a direct consequence of changes in energy balance. Indicators based on the SST projection show the spatial scale and magnitude of future changes, as well as the difference between scenarios. This Chapter considers first the future evolution of SST by analyzing model projections, its consequence on the Indo-Pacific Warm Pool (an ocean feature playing an important role in global circulation), the occurrence of annual periods of higher warming potentially harmful to coral (Degree Heating Month Alert Level 2), and consequences of global warming on sea ice in the Polar Regions.

Projections of SST were obtained by computing the ensemble mean of model outputs under scenarios MM and BAU (see Methods 4.2.3). The result of the operation is a time-series of ocean surface temperature, grouped by decades, from 2010 to 2059 (which is the last year of decade 2050): the number of model averages per grid cell is in the final product, as well as the minimum-maximum amplitude between model averages. Figure 4.13 shows the sea surface temperature at the beginning of the projection under BAU, as the average of year 2010.

Figure 4.13. Initial value of the sea surface temperature projection ensemble mean, as the average of year 2010, for BAU (RCP 8.5)

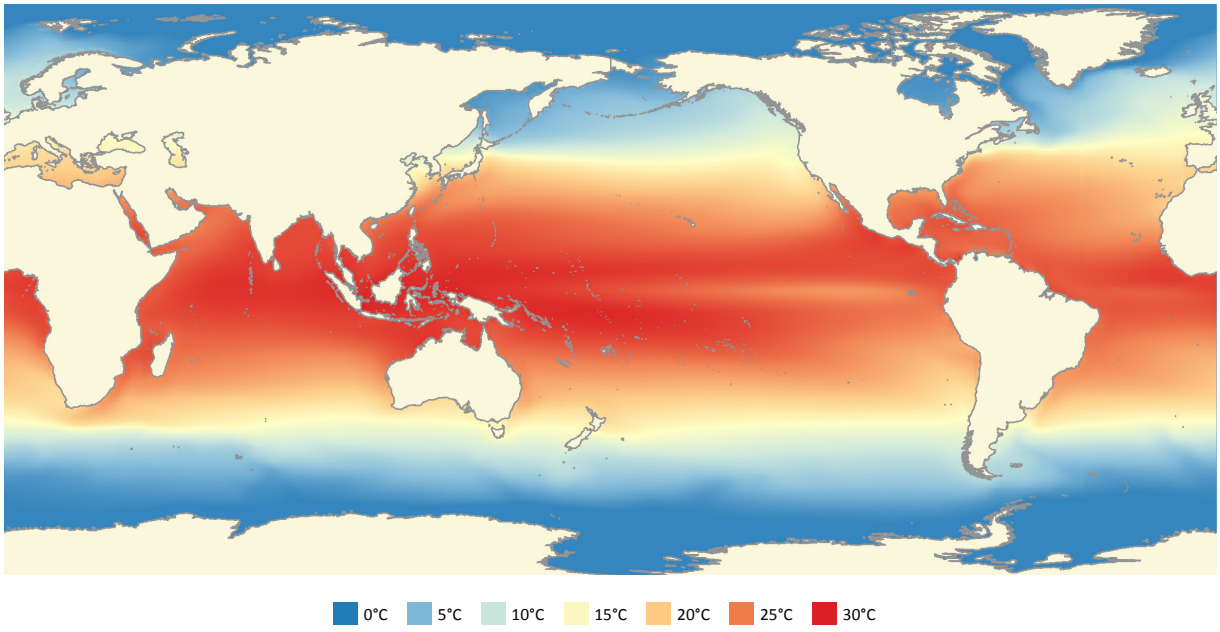

Figure 4.14 illustrates intrinsic ensemble mean variability, as the standard deviation for a given date. The colour bar was stretched to clearly show the existence of difference among the models, though this difference is in general rather low. The ensemble mean standard deviation remains below 0.5°C in most of the ocean, and a large fraction is even below 0.3°C. This spread among models is below the projected increase of temperature. Actually the expected

increase in temperature is expected to be not less than 0.75°C, and in general beyond 2°C for BAU around 2050 (see Figure 4 analysed in this section). The small spread has a spatial consistency and seems to correspond to differences in the modelling of the ocean local dynamic and thermodynamic features. These small differences among models justify the need to consider an ensemble mean, rather than a single model, which can smooth local discrepancies when carrying a global study.

However, some specific areas show higher spread of the model outputs, reaching up to 1.2°K, shown in red on Figure 2. Such differences between the models are generally found close to the shores and explained by the different representations of the coastline in the various models grids. Some features, generally ocean currents, such as in the North Atlantic, however, show higher magnitude of differences, which would deserve further analysis from the research team developing the models.

Figure 4.14. Standard deviation of the Sea Surface Temperature ensemble mean, 2050, July, BAU (RCP 8.5)

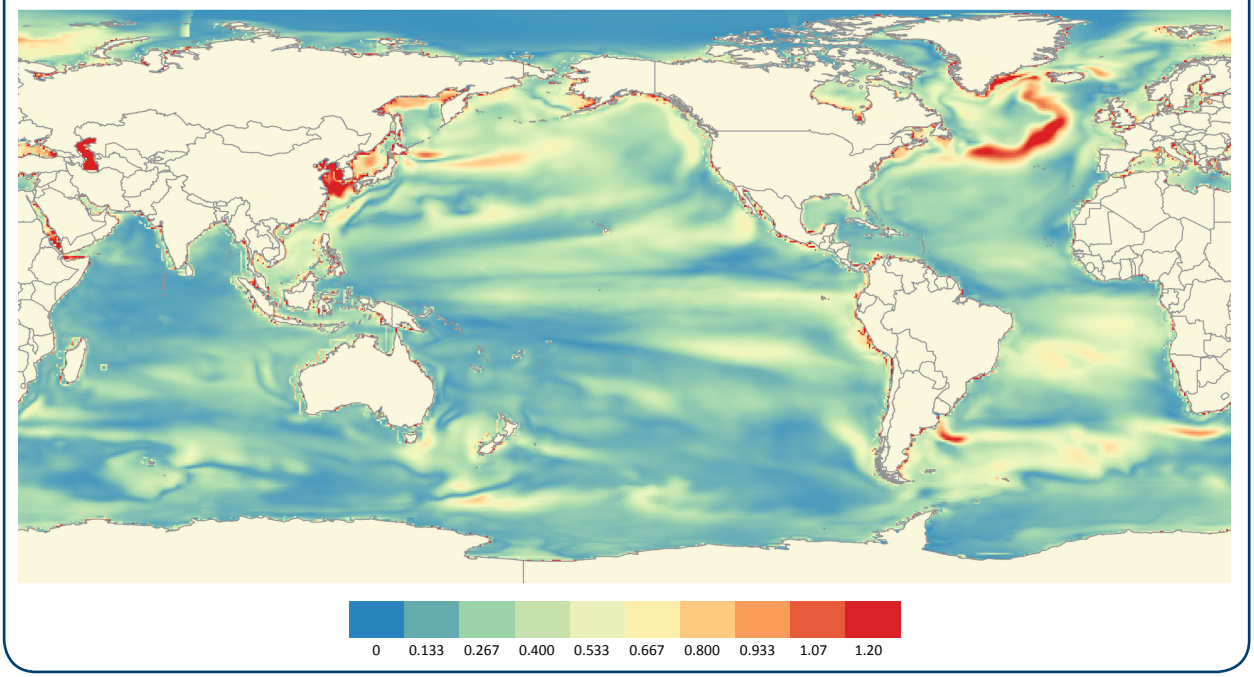

Computing the difference between the decadal temperature average for decade 2050 (2050-2059) and the climatology (period 1971 to 2000) shows that the entire ocean may experience a temperature increase, for both scenarios MM (**Figure 4.15**) and BAU (**Figure 4.16**). Some features, easily distinguished under MM (Figure 3) , show a local increased warming: in the northern Pacific, in the northern Atlantic close to the North America shores and, around European countries. This increased warming can be explained by local forcing (expressed in the scenarios) and by transportation through ocean circulation. Some features of the global circulation, such as the counter equatorial current also exhibit an increased warming. Both scenarios show that the Northern Hemisphere could have the highest temperature increase by 2050, with up to a 3°C increase compared to the climatology.

The Moderate Mitigation (MM) and Business-as-usual (BAU) scenarios are both projections of the future sea surface temperature (SST), with respect to the 1971-2000 climatology. The difference between the two scenarios, which can be linked to the uncertainty of the projections, is shown in **Figure 4.17** and indicates a SST difference below 0.5C over most of the ocean. Some rare locations (for example East of Japan) show a warming of about 1°C more for BAU than MM. Most of the Southern Seas, around the Antarctic show a very low difference (below 0.2°C). For some rare exceptions (for example in Central Atlantic), MM may result in a slightly higher increase than BAU.

Figure 4.15. Temperature difference between average temperature in decade 2050 and climatology (average temperature between 1971 and 2000), under MM (RCP 4.5).

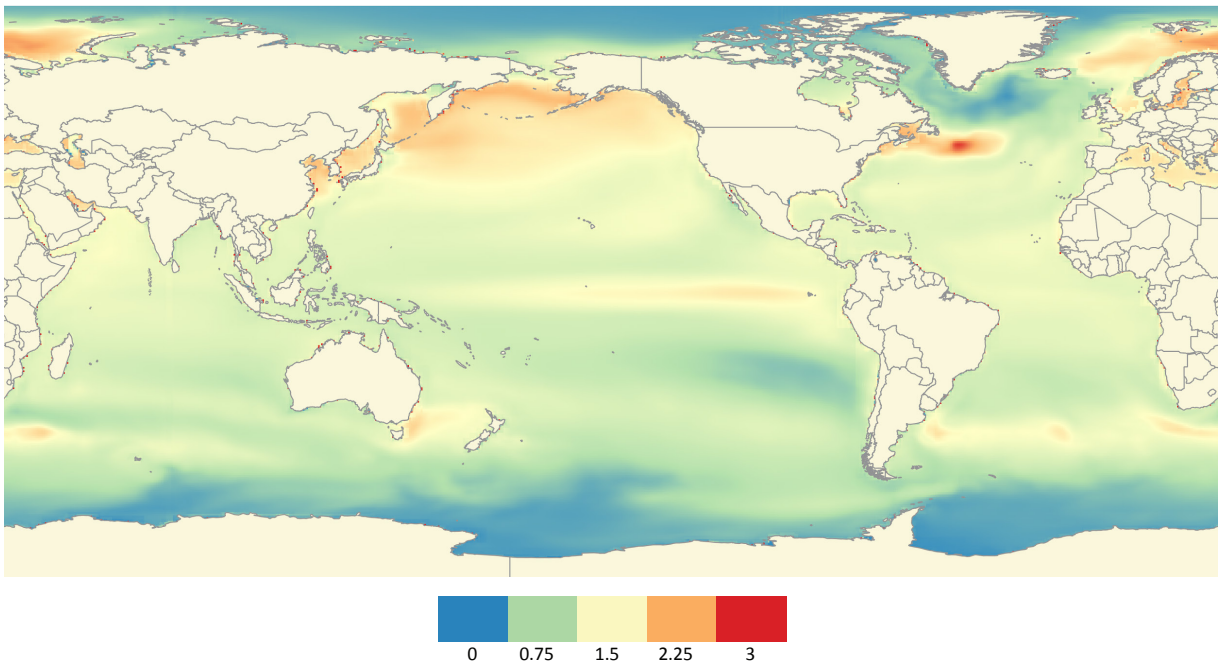

Figure 4.16. Temperature difference between average temperature in decade 2050 and climatology (average temperature between 1971 and 2000), under BAU (RCP 8.5).

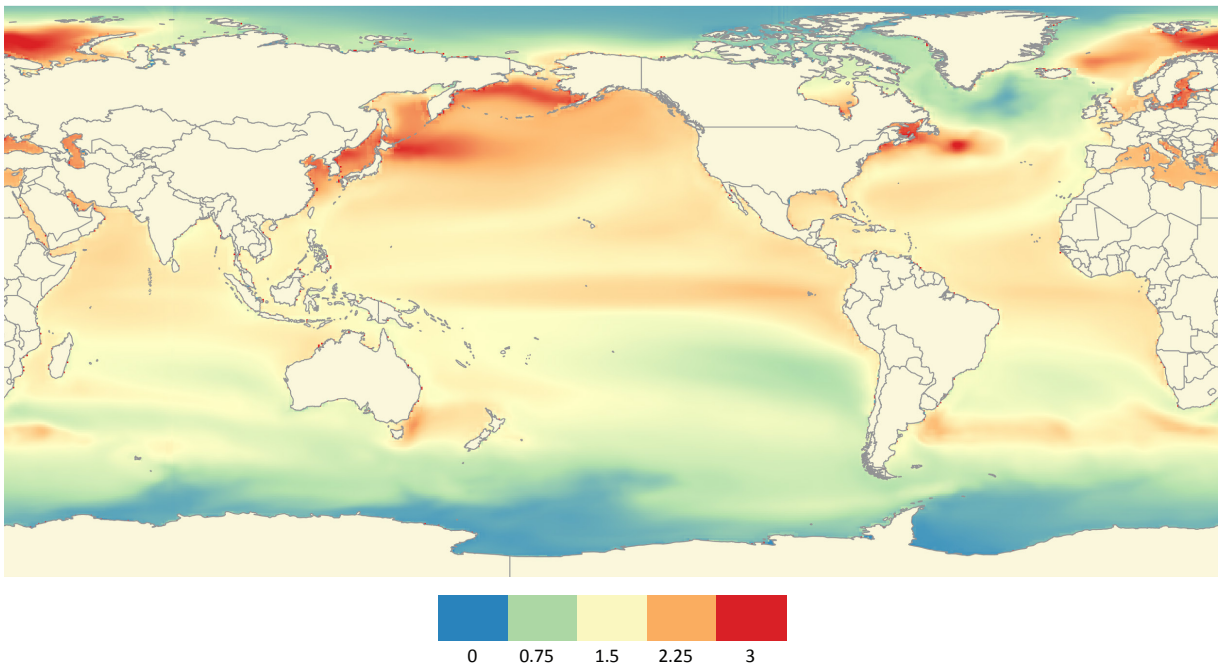

Figure 4.17. Comparison of SST increase under BAU (RCP 8.5) and MM (RCP 4.5) as a temperature difference, for decade 2050 compared to the climatology.

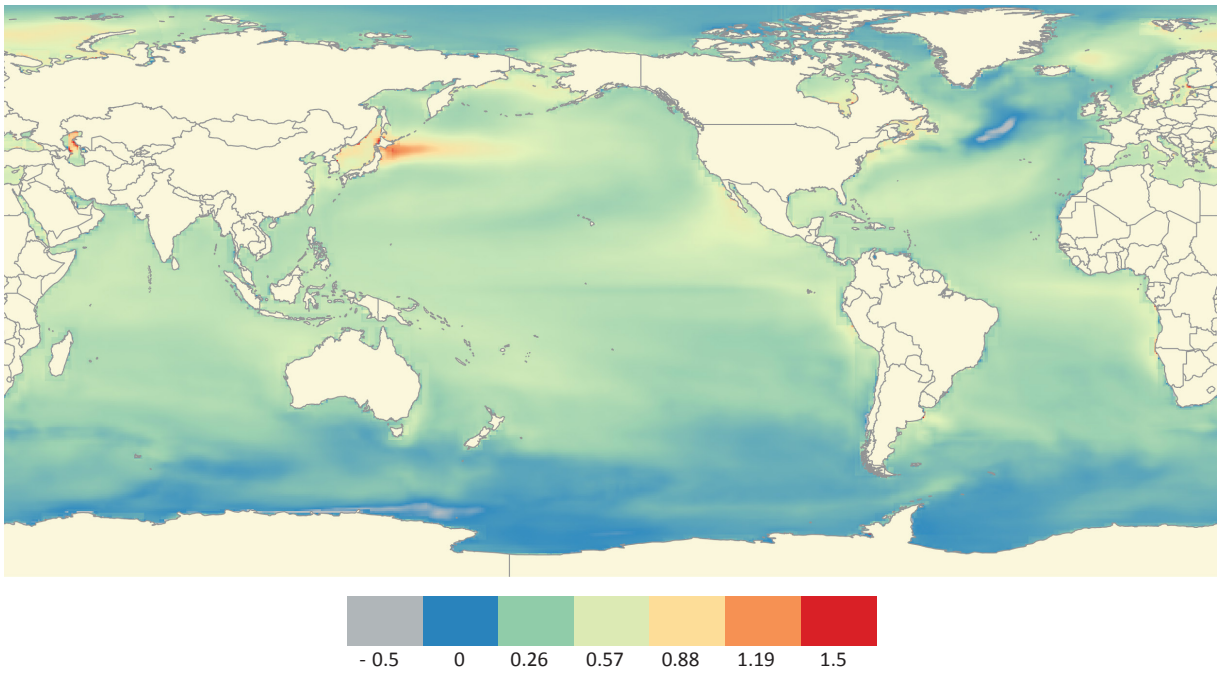

Warm Pools

The tropical Indo-Pacific Warm Pool (IPWP) possesses the warmest open ocean SST and the largest precipitation on the planet. The large scale heating over the tropical warm pools play a critical role in the global redistribution of heat, moisture, and momentum, resulting in a balancing of the global heat budget (for example Webster 1994; Lin and Johnson 1996). A considerable number of studies have shown the relations between the Western Pacific Warm Pool (WPWP) year to year variation in temperature and size and the El Niño Southern Oscillation (ENSO) and to global climate changes (for example Xiao-Hai et al. 1992; Wang and Mehta, 2008; Xie et al. 2014, Xiao-Han et al. 1992). The surface temperature time-projection projects the potential growth and warmth of the IPWP between MM and BAU. An important change in the size and temperature of the warm pool will result in atmospheric changes at regional and global scales, change in global circulation, and probably an impact on ecosystems. These consequences are not analysed in this Chapter, the presented material being an indicator of change available for further studies.

The IPWP is shallow, consistently warm water. Within scientific literature, several values of the iso-contour of temperatures delineating the IPWP and WPWP were found. This study uses 28°C, justified by Wyrtki (1989). However, the generated data contains a projection of the inner temperature, allowing comparison to more restrictive studies using 29°C as the definition of the Warm Pool. The colour ranges in the illustrations allow visualising areas corresponding to different definitions. Moreover, the whole globe was used to identify areas to which the same definition applies: further illustrations show that the current area identified as the IPWP is expected to expand across the Pacific, and that a similar area is found at the same latitude in the Atlantic.

The IPWP is the portion of the ocean where the annual average temperature remains above 28°C. The time projection of the IPWP in terms of occupied surface and temperature was estimated on the CMIP5 ensemble mean of TOS.

Historical outputs of models, corresponding to models run before 2006, without any radiative forcing (and therefore irrespective of any RCP), were used to generate a climatology. For the period 1971 to 2000, a monthly average of the models SST was computed. The definition of the Warm Pool was applied to this climatological year. The resulting "climatological Warm Pool" is a reference state for assessing the Warm Pool warming.

The SST climatology based on models (1971 to 2000) shows an IPWP with temperatures mostly between 28°C and 28.5°C. There is a gradient of increasing temperatures when moving from the outside delineation toward its "core", with a peak of temperatures around 29.5°C in the Western Pacific part of the IPWP, near the Philippines and Papua New Guinea (**Figure 4.18**). Some parts of the Eastern Pacific, close to Mexico and the Eastern Atlantic, along Gulf of Guinea, also show waters with a temperature signature corresponding to our definition of a Warm Pool 28°C). The same figure shows that the outline corresponding to a temperature superior or equal to 28.5°C, sometimes found in the literature, is very close to the 28°C definition.

The current delineation of the Warm Pool is expected to increase in surface, under any scenario, as shown in the next figures. For this reason, a concept of a "Global" Warm Pool is introduced in this chapter, corresponding to any water matching the IPWP definition; this term was used rather than "Tropical Warm Pool" which is often used in the literature in lieu of IPWP. The rationale is not ecological, but rather corresponds to the fact that the permanently warm waters are expect to grow in area and eventually represent a continuous region around this equator. Further in this text, the distinction is made between the "Global" Warm Pool, corresponding to any water matching the definition, and the IPWP corresponding to the waters in the Indian Ocean and Western Pacific.

Figure 4.18. Spatial extension and temperature of the IPWP, according to a historical run of models (no radiative forcing), for the period 1971 to 2000.

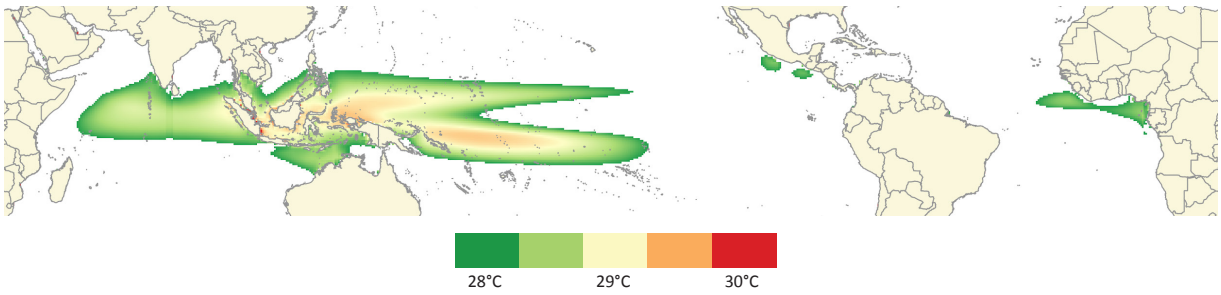

The projection of the Global Warm Pool to the end of decade 2050 (year 2059) is framed by scenarios MM and BAU. Both scenarios show a spatial extension of the IPWP to the Eastern African coast, in the Bay of Bengal and across the Pacific Ocean toward Central America. In addition, the overall temperature significantly increases, above 29.5°C for the largest part of the IPWP.

A similar pattern of expansion and warming is shared between MM and BAU, the first being more pronounced. BAU features the development of a large Warm Pool across the Atlantic Ocean, connecting the African Western Coast to Brazil.

The SST temperature increase forecast by the models under both scenarios allows the growth of the IPWP as well as the Global Warm Pool (**Figure 4.20**). To compare both scenarios, the areas were expressed as a fraction to the model estimate in 2010 (shown as dots for the IPWP in **Figure 4.20**, starting at one in 2010, only the regression lines for BAU has a bias below one). The climatology was not used as a reference to ensure extracting the progression, as it is a 30 year based estimate, while each point on **Figure 4.20** is an annual estimate.

Figure 4.19. IPWP projection for year 2059, under MM (RCP 4., top) and BAU (RCP 8.5, bottom).

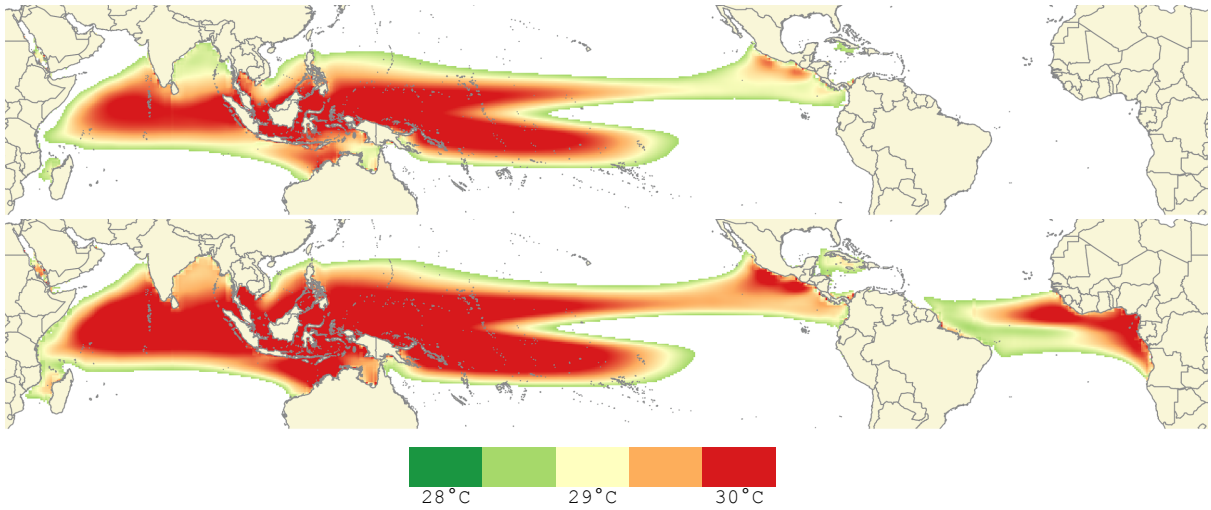

The time-series of the forecast IPWP shows an almost linear progression of the area of the IPWP (**Figure 4.20**) under both scenarios. The model outputs show a strong linear progression of the area with only inter-annual fluctuations. The Global Warm Pool (shown only for BAU) also grows linearly and follows a similar trend.

The relative surface increase is about 3 per cent per year for the Indo-Pacific area, under BAU. According to MM, the annual increase of the IPWP would be about 1.8 per cent a year. In spite of limited emissions in MM, the projected surface increases continuously and linearly, only slowing the process of the expansion by about two decades with respect to BAU.

Figure 4.20. IPWP relative area (area/area in 2010), for BAU (RCP 8.5) and MM (RCP 4.5). The continuous lines show linear fits.

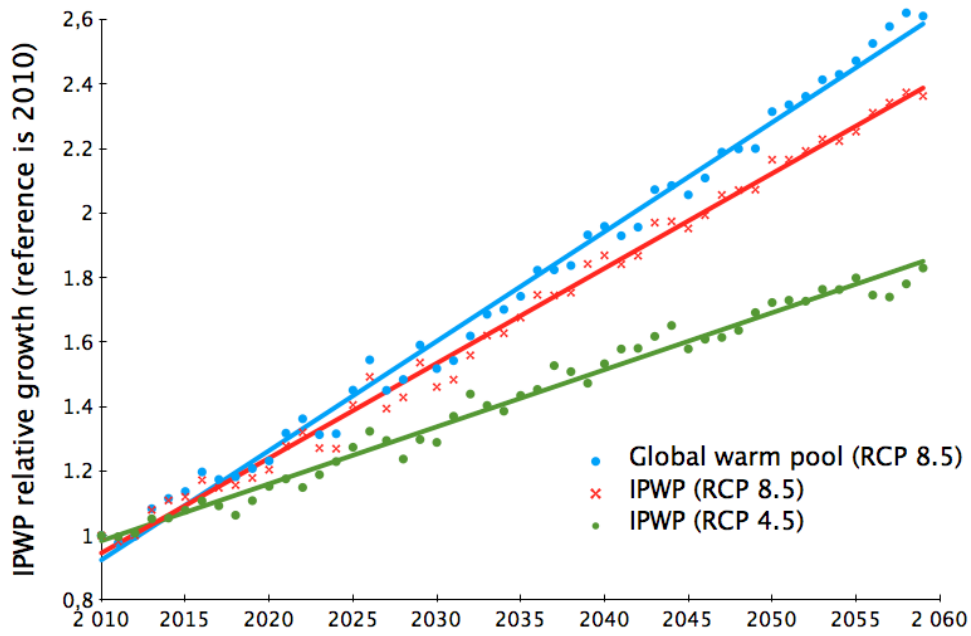

Areas possibly affected by the expansion of the Warm Pool at global scale, according to BAU, between 2010 and 2059 are shown in **Figure 4.21**. The Warm Pool expands to Northern Hemisphere latitudes, towards the Gulf of Bengal and to Taiwan in the Pacific. It also expands to the West to the Eastern coasts of Africa (from Somalia to Tanzania). Towards the South, it expands to the Gulf of Carpentaria. It also significantly expands into the Pacific connecting to Central America, along the northern path of the ENSO. The simulation also shows a significant expansion in the Atlantic, almost connecting the Gulf of Guinea to South America.

Figure 4.21. IPWP expansion between climatology (orange area) and 2059 (gray area), RCP 8.5.

In **Figure 4.22**, the IPWP temperature increases by at least 0.8°C in its core area between 2010 and 2050. The temperature increase is more important on the edges of the IPWP, reaching 1.6°C. The gray area corresponds to waters that become part of the IPWP once it expands. As the gray area does not match the warm pool definition at the initial date of 2010, no temperature increase can be defined consistently with the rest of the initial warm pool. The highest increase in temperature for the warm pool (as delineated in the 2010 initial period) is found across the coolest areas (**Figure 4.19**), whereas the warmest areas (closest to the central region of the Warm Pool, around Indonesia and Malaysia) gain less temperature.

Figure 4.22. Temperature increase of the initial warm pool area, for BAU (RCP 8.5).

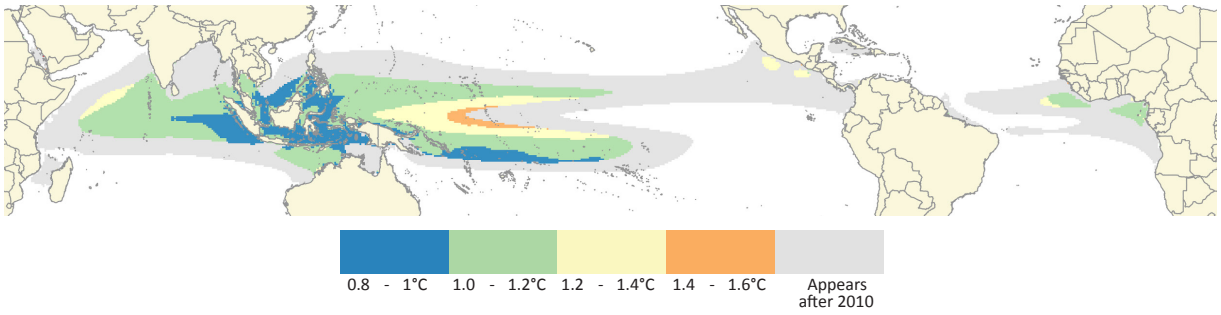

Degree Heating Month and Thermal stress

In tropical regions, species are adapted to stable temperatures, in contrast with higher latitudes where seasonality is more pronounced. The increase in temperature is not expected to be constant and smooth, but rather to show peaks of temperature within the year, which may result in a stress for the tropical species accustomed to more stable conditions. Chapters 5.4 and 5.5 investigate in details the impact of ocean warming and acidification on the habitat and biological functions of corals and pteropods.

A risk indicator was used to represent the possible future impact on those species; combining temperature increase and acidification (see Chapter 4.4 for projections of acidification). The thermal stress indicator corresponds to the accumulation, in a four-month time-frame, of degrees Celsius above the local "normal" temperature, which is a good proxy of the stress on corals (Donner 2009). This indicator, named DHM for "Degree Heating Month", shows a significant level of alert if the accumulated excess of temperature goes beyond 2 °C in 4 months, known as an "Alert Level 2", and representing a potentially harmful situation for corals in hot water. The potential risk was expressed by the frequency of exposure (in a decade) to an Alert Level 2. Chapter 5.4 analyses the impact of heat stress and ocean acidification on coral reefs. The concept of a 2°C Alert as an indicator of risk makes sense for species living in warm equatorial waters were the seasonal amplitude is not expected to be as important as it is in temperate regions. Outside of warm waters coral reef areas, this indicator gives a sense of the repetition of warm peaks in a decade.

The projection of DHM Alert Level 2, under BAU, for decade 2050 shows that an annual Alert Level 2 affects most seas. A value of 10, shown in red in **Figure 4.23**, means that this alert occurred every year in the decade. Some regions may be free of any Alert Level 2, such as a fraction of the North Atlantic, the Southern Arctic Ocean, and some areas in the South Pacific (where a large fraction of the ocean also shows low frequency of occurrences).

For the same decade, and using MM, the occurrence of thermal stress Level 2 appears to be permanent (with ten annual occurrences in the decade). However, at a global scale, many regions would be spared which such a scenario. The decadal evolution, from 2020 to 2050 under MM is outlined in the Notes on Methods 4.2.3.

The two scenarios suggest a range of climate response where a large fraction of the ocean is exposed to an Alert Level 2 every year, suggesting that Alert Level 2 is *likely* to occur in those regions of the globe.

Figure 4.23. Frequency of DHM Level 2 Alert, for decade 2050 (2050-2059), under BAU (RCP 8.5).

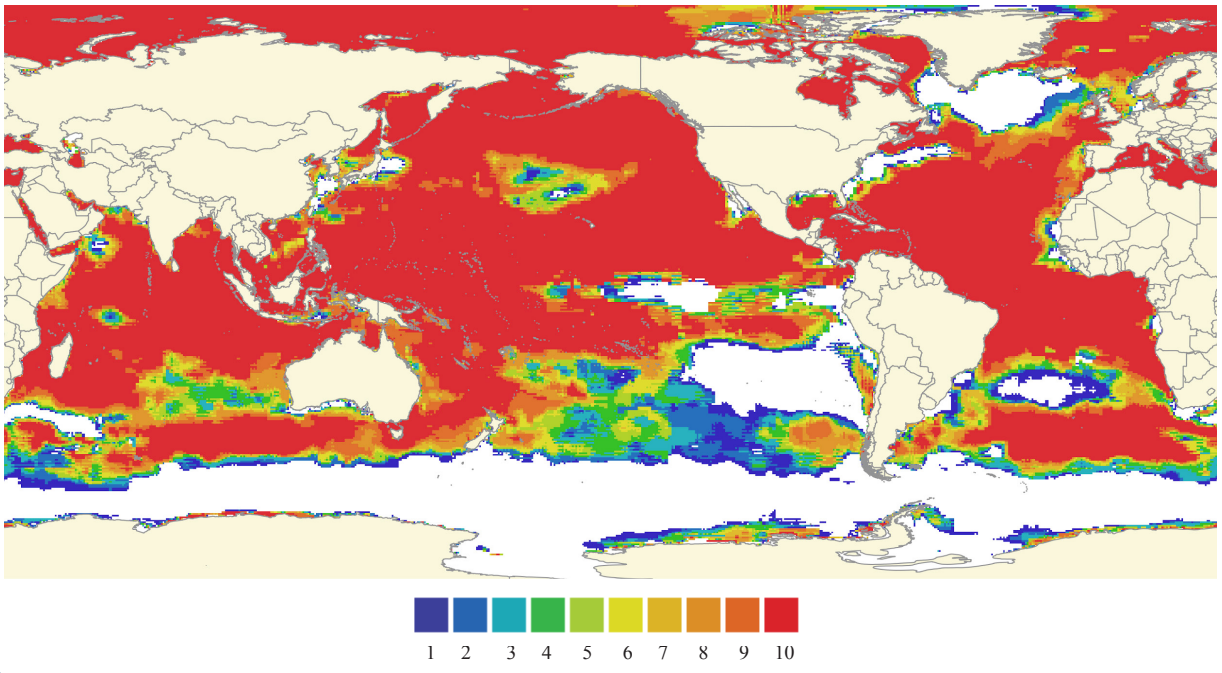

Figure 4.24. Frequency of DHM Level 2 Alert, for decade 2050 (2050-2059), under MM (RCP 4.5).

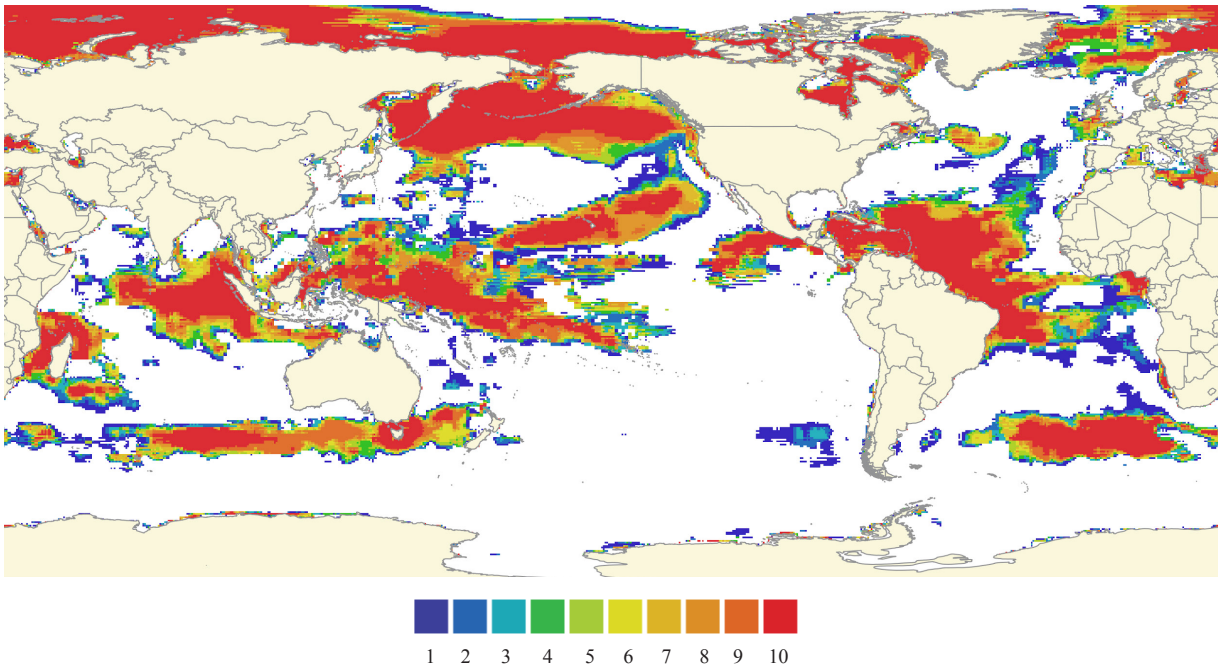

Polar Sea Ice

The Polar Regions are often perceived as cold, desolate and virtually devoid of all animals and plants. However, this is not the case. Every summer, a short period of sunshine (three months only) allows an explosion of life in surface waters. Under the ice, tiny algae (diatoms) capture the little light available to survive. Zooplankton also proliferates here and is an essential link in the Arctic food chain (see Chapter 5.3), which in turn feeds small invertebrates, small carnivores and the upper stages of the ecosystem web including fish, birds, whales and other marine mammals.

Sea ice also plays an important role as a barrier, forbidding access to ships during the whole winter. From a physical point of view, Polar sea ice cover reflects solar energy to space, whilst insulating the ocean from heat loss. Regional climate changes affect the sea ice characteristics and these changes can feed back on the climate system, both regionally and globally.

Sea ice cover in the Polar Regions is thus a visible signature of seasonal warming, as it expands with steeply decreasing temperatures in winter and decreases with the warmer air temperature of summer. The total extent of sea ice at both Poles is a major indicator of the effect of the global warming. However, the impacts from climate change and threat of human activities on the two Poles are not equal. International treaties protect the Antarctic, limiting human activities and settlement, whereas the Arctic is exposed to a larger human footprint. Populations (mostly in developed countries) living in Boreal regions exert a significantly higher pressure due to their close proximity to the Arctic. Decreasing Arctic sea ice cover may increase access to this Polar Region and in consequence, increasing human activities that potentially degrade the so far pristine waters. This area also lacks the international protection laws adopted for the Antarctic (see Chapter 3). For these reasons, this Chapter emphasises the Arctic more than the Antarctic.

Arctic sea ice cover varies seasonally, between 6×10^6 km^2 (2.3×10^6 square miles) in the summer and 15×10^6 km^2 (5.8×10^6 square miles) in the winter (Comiso and Nishio, 2008; Cavalieri and Parkinson, 2012; Meier et al. 2012). Mainly, the summer ice cover is confined to the Arctic Ocean basin and the Canadian Arctic Archipelago, while winter sea ice reaches south as far as 44°N, into the peripheral seas. In September, at the end of Northern Hemisphere

summer, the Arctic sea ice cover consists of the ice that survived the melt period. **Figure 4.25** shows that the Arctic sea ice available at summer's end has been decreasing since 1979. The inter-annual variability is largely determined by the extent of the ice cover in the peripheral seas in winter and by the ice cover that survives the summer melt in the Arctic Basin.

Figure 4.25. Arctic sea ice area estimates from satellite imagery, by NSIDC. The sea ice grows and shrinks each year, the minimum in September. The trend of the decrease of the area observed in September is clearly negative (about 10×10^3 km² loss per year.

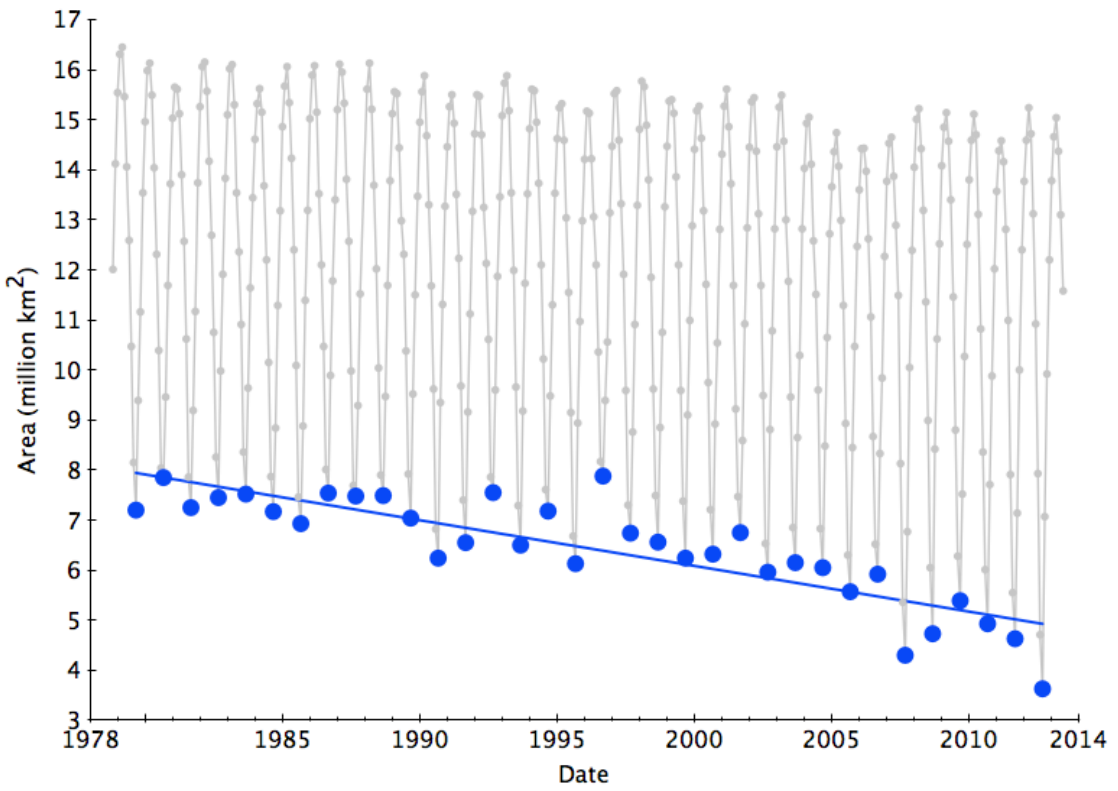

The average rate of ice loss from the Antarctic ice sheet has *likely* increased from 30 [–37 to 97] giga tons per year over the period 1992–2001 to 147 [72 to 221] giga tons per year over the period 2002 to 2011. There is *very high confidence* that these losses are mainly from the northern Antarctic Peninsula and the Amundsen Sea sector of West Antarctica (IPCC, 2014).

The annual mean Arctic sea ice extent decreased over the period 1979 to 2012 with a rate that was *very likely* in the range 3.5 to 4.1 per cent per decade (range of 0.45×10^6 to 0.51×10^6 km² per decade), and *very likely* in the range 9.4 to 13.6 per cent per decade (range of 0.73×10^6 to 1.07×10^6 km² per decade) for the summer sea ice minimum (perennial sea ice). The average decrease in decadal mean extent of Arctic sea ice has been most rapid in summer (*high confidence*); the spatial extent has decreased in every season, and in every successive decade since 1979 (*high* confidence, IPCC, 2014).

IPCC WGI reported the projection of the sea ice extent using CMIP5 models the closest to the climatological mean state and 1979 to 2012 trend of the Arctic sea ice. The future sea ice extent under BAU (respectively MM) was estimated using 5 models (respectively 3). Both scenarios frame the future possible sea ice extent (see Figure 4-26). BAU predicts that the Arctic could be found in ice free condition after 2050, with less than 1×10^6 km² of sea ice in 5 consecutive years. MM also predicts ice free conditions beyond 2050, but with a larger uncertainty making the ice free condition not certain under this scenario. MM indicates that lowering the radiative forcing down to 2.6 W.m²

could significantly hamper the process and allow a stabilisation of the sea ice extent around 2.5×10^6 km^2 by 2050 without significant loss beyond. However, these simulations show large uncertainty.

Figure 4.26. Changes in sea ice extent as simulated by CMIP5 models over the second half of the 20th century and the whole 21st century under RCP2.6, RCP4.5 (MM), RCP6.0 and RCP8.5 (BAU) for (left) Northern Hemisphere September, (right) Southern Hemisphere February. The solid curves show the multi-model means and the shading denotes the 5 to 95 per cent range of the ensemble. The vertical line marks the end of CMIP5 historical climate change simulations. One ensemble member per model was taken into account in the analysis. Sea ice extent was defined as the total ocean area where sea ice concentration exceeds 15 per cent and was calculated on the original model grids. Changes are relative to the reference period 1986–2005. The number of models available for each RCP was given in the legend. Also plotted (solid green curves) were the satellite data of Comiso and Nishio (2008, updated 2012) over 1979–2012. Source: IPCC AR5.

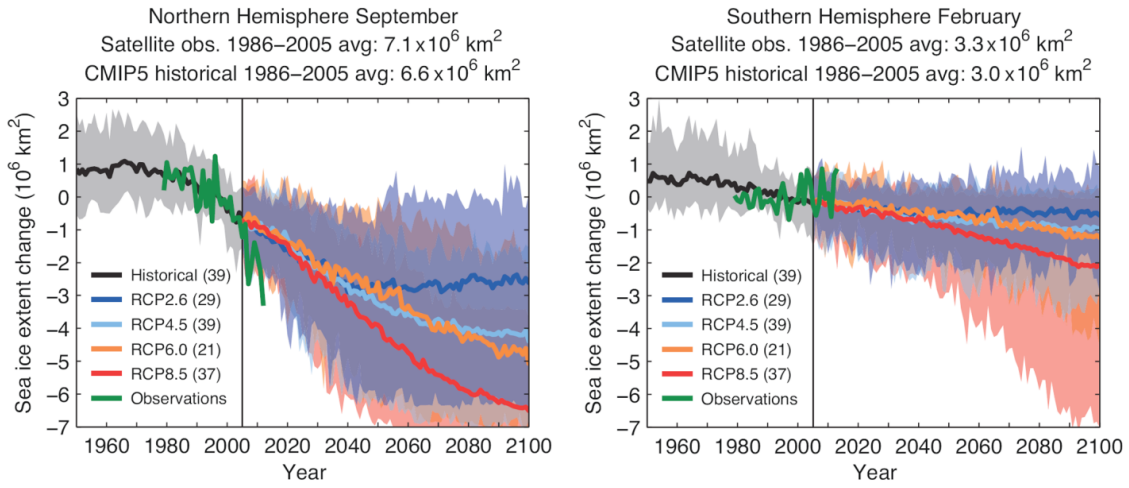

There is *medium confidence* from reconstructions that over the past three decades, Arctic summer sea ice retreat was unprecedented and SSTs were anomalously high in at least the last 1,450 years (IPCC, 2014).

It is *very likely* that the annual mean Antarctic sea ice extent increased at a rate in the range of 1.2 per cent to 1.8 per cent per decade (range of 0.13×10^6 to 0.20×10^6 km^2 per decade) between 1979 and 2012. There is *high confidence* that there are strong regional differences in this annual rate, with extent increasing in some regions and decreasing in others (IPCC, 2014). Considering the low rate of growth observed on the last decades and the models forecast showing some decrease (though less drastic than for the Arctic), the future evolution of the Antarctic sea ice is difficult to state with certainty.

Discussion and conclusions

The SST projections show that the ocean will become warmer by 2050, for both MM and BAU scenarios, with a difference smaller than 1°C in most regions. The Northern Hemisphere latitudes are expected to experience the most warming, accumulating up to 3°C under BAU.

This generalised increase in temperature is *likely* to affect the Indo-Pacific Warm Pool, causing it to become significantly larger and warmer. Such an evolution may influence the global atmospheric circulation, by increasing the thermal forcing.

the extent to which the projected temperature exceeds that observed between 1971 and 2000 is an indicator of the thermal stress to which living organisms may be exposed. This indicator shows that by 2050, most of the ocean should warm by more than 2°C in 4 months, above the climatology, every year, which is threatening both coral reefs (Chapter 5.4) and species such as pteropods (Chapter 5.5).

The mean Arctic sea ice extent decreased over the period 1979 to 2012 at a yearly rate of about 3.5 to 4.1 per cent per decade (IPCC, 2014). The Northern Hemisphere summer sea ice, the perennial ice remaining at the end of the summer melting process, decreased by about 9.4 to 13.6 per cent per decade for the same period (IPCC, 2014). According to the projections, the extent of the summer sea ice will continue decreasing to 2050 and beyond.

4.2.3 Notes on Methods

Processing Sea Surface Temperatures (SST) projections ensemble mean

The CMIP5 Sea Surface Temperatures (SST) model projections correspond to the coupled ocean-atmosphere general circulation model (OAGCM) outputs named Temperatures of Ocean Surface (TOS) with a monthly time-step (12 values per year, from 2006 to 2100), for MM and BAU (Combal and Caumont, 2016, in press). The computed data are available for download (Combal 2014a).

For a given RCP, some models can have different sets of input parameters (called input ensemble), numbered r1i1p1, r1i1p2, etc, corresponding to different input settings, resulting in an output for each rXiYpZ input. Variable 'TOS' is provided by 86 combinations of models and input ensembles (see below).

The different outputs of a single model were first averaged to compute an ensemble mean with equal weight for each model. The resulting averaged models outputs, 1 average per model, are then re-gridded to a common grid, defined as a regular grid, with a spatial resolution of ½ ° in latitude per ½ ° in longitude, from 0° to 360° in longitude, and -85° to 85° in latitude. Because of the difference in the spatial gridding, and difference in the land mass representation, some grid points were not represented in all models. Then, the re-gridded averages were averaged all together with the same weight (Oldenborgh et al. 2013).

The averaging operations are grid-cell and time independent, which means that the averaging operator is not applied along the space and time dimensions, only in-between the different models values for the same place and time.

Table 1: List of models providing "TOS" variables, for ocean SST projections, analysis, and the different input ensembles used:

ACCESS1-0	r1i1p1	FIO-ESM	r1i1p1 r2i1p1 r3i1p1
ACCESS1-3	r1i1p1	GFDL-CM3	r1i1p1
bcc-csm1-1	r1i1p1	GFDL-ESM2G	r1i1p1
bcc-csm1-1-m	r1i1p1	GFDL-ESM2M	r1i1p1
BNU-ESM	r1i1p1	GISS-E2-H	r1i1p1 r1i1p2 r1i1p3
CanESM2	r1i1p1 r2i1p1 r3i1p1 r4i1p1 r5i1p1	GISS-E2-R	r1i1p1 r1i1p2 r1i1p3
CCSM4	r1i1p1 r2i1p1 r3i1p1 r4i1p1 r5i1p1 r6i1p1	HadGEM2-AO	r1i1p1
CESM1-BGC	r1i1p1	HadGEM2-CC	r1i1p1 r2i1p1 r3i1p1
CESM1-CAM5	r1i1p1 r2i1p1 r3i1p1	HadGEM2-ES	r1i1p1 r2i1p1 r3i1p1 r4i1p1
CESM1-WACCM	r2i1p1 r3i1p1 r4i1p1	inmcm4	r1i1p1
CMCC-CESM	r1i1p1	IPSL-CM5A-LR	r1i1p1 r2i1p1 r3i1p1
CMCC-CM	r1i1p1	IPSL-CM5A-MR	r1i1p1 r2i1p1 r3i1p1
CMCC-CMS	r1i1p1	IPSL-CM5B-LR	r1i1p1
CNRM-CM5	r10i1p1 r1i1p1 r2i1p1 r4i1p1 r6i1p1	MIROC5	r1i1p1
CSIRO-Mk3-6-0	r10i1p1 r1i1p1 r2i1p1 r3i1p1 r4i1p1 r5i1p1 r6i1p1 r7i1p1 r8i1p1 r9i1p1	MPI-ESM-LR	r1i1p1
EC-EARTH	r10i1p1 r11i1p1 r12i1p1 r14i1p1 r1i1p1 r2i1p1 r3i1p1 r6i1p1 r7i1p1 r8i1p1 r9i1p1	MPI-ESM-MR	r1i1p1
		MRI-CGCM3	r1i1p1 r2i1p1 r3i1p1 r4i1p1
		NorESM1-M	r1i1p1
		NorESM1-ME	r1i1p1

Computing Degree Heating Month (DHM)

The DHM computation follows the definition in Donner (2007), although different inputs were used. The SST climatology used is the so-called Reynolds data set (climatology for the period 1971-2000), and the model time projections of SST was derived from CMIP5 ensemble means, as described in Section 2.

The SST climatology $SST^{R}(t)$, commonly known as "Reynolds climatology", is obtained from NOAA/OAR/ESRL PSD, Boulder, Colorado, USA (Data from Xue, NOAA). The analysis uses in situ and satellite SST. The climatology spans the period 1971 to 2000, with a time resolution of 1 month and a spatial resolution of 1°x1° (Reynolds et al. 2002). In the notation $SST^{R}(t)$, t is a month in the range 01 to 12 (from January to December).

The time projection of the Models $\underline{TOS}(t)$ correspond to the CMIP5 models ensembles, for scenarios RCP 8.5 and RCP 4.5. Datasets are available for download (Combal 2014b, Combal2014c).

The ensemble means of models' projections were adjusted to the climatology in order to ensure that both the model outputs and the climatology were consistent for the period 1971-2000. The "TOS climatology" of the model ensemble mean $\underline{TOS}(t)^{clim}$ for the period 1971-2000 were computed with CMIP5 "historical values", which do not depend on the forcing scenarios RCPs (Taylor et al. 2009), as they start in 2006.

The monthly difference $\Delta(t)$ between the model ensemble mean projections and the model climatology, $\Delta(t) = \underline{TOS}(t) - \underline{TOS}(t)^{clim}$, corresponds to the variation of the ensemble means projections around $\underline{TOS}(t)^{clim}$. This variation $\Delta(t)$ was added to the Reynolds climatology to obtain corrected model projections: $\underline{TOS}(t)^{corr} = \mathrm{SST}^{R}(t) + \Delta(t)$.

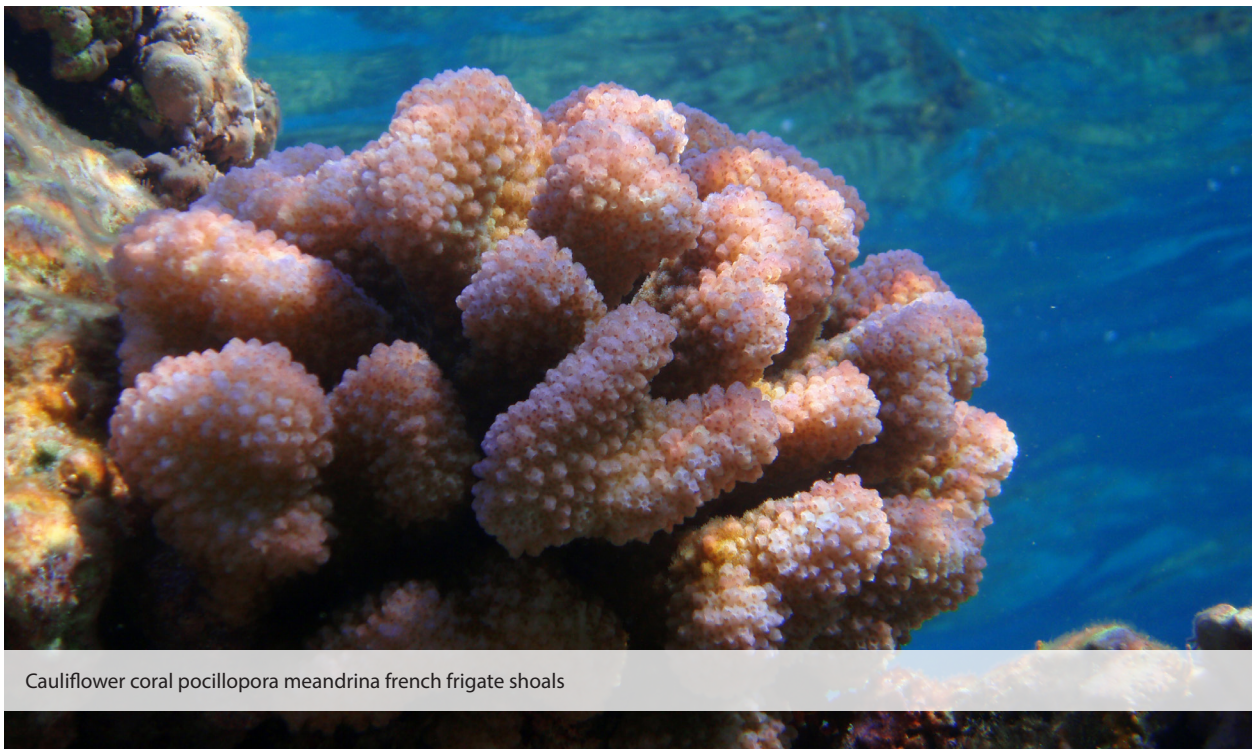

Cauliflower coral pocillopora meandrina french frigate shoals

DHM represents the accumulation of temperature beyond the maximum observed in the climatology for this point maximized with the climatology standard deviation observed at the date of the climatology maximum. Only positive differences are accumulated.

A yearly DHM corresponds to the maximum 4-month-DHM observed in the year.

$$DHM = \sum_{i=t}^{t-3} \left(\underline{SST}(i)^{corr} - \left(SST^{R}_{max}(t) + \sigma_{max} \right) \right) > 0$$

The DHM corresponds to a Risk Level 2 if its value is equal or above 2°C. The "Level 2 Frequency" corresponds to the number of occurrences of yearly Level 2 in ten years.

Reynolds climatology and the CMIP5 ensemble means do not represent the coastline in the same way. The ensemble means have a finer spatial resolution, and the Reynolds dataset shows values over the land for its root mean square (the dataset was spatially smoothed, ignoring discontinuity imposed by land mass). As a result, some locations close to small islands or some irregular coast, existing in both Reynolds and the ensemble means, may ignore the land mass in one case and not the other. As a result, the same pixel may show dramatically different time-series, resulting in an isolated erroneous high frequency of DHM Level 2.

In a first step, these isolated pixels were detected from an image where the DHM Frequency Level 2 was null or minimal (typically RCP 4.5, 2020). Once their locations were found, their values were replaced in all the other dates and scenarios with the most frequent values in their immediate surrounding (in a 3x3 window).

Decadal evolution of thermal stress under scenario RCP 4.5

Under scenario RCP 4.5, a Frequency Level 2 was not visible before 2040 (Figure 4-27 and Figure 4---28). Within decade 2040, some impact is visible, with a maximum frequency of eight years in the decade. In decade 2050 (Figure 4-29), the impacted areas expanded slightly, and the frequency reaches its maximal value of 10 years per decade.

Figure 4.27. Frequency (number of years of occurrence per decade) of DHM Alert Level 2, 2030 (2030-2039), MM (RCP 4.5).

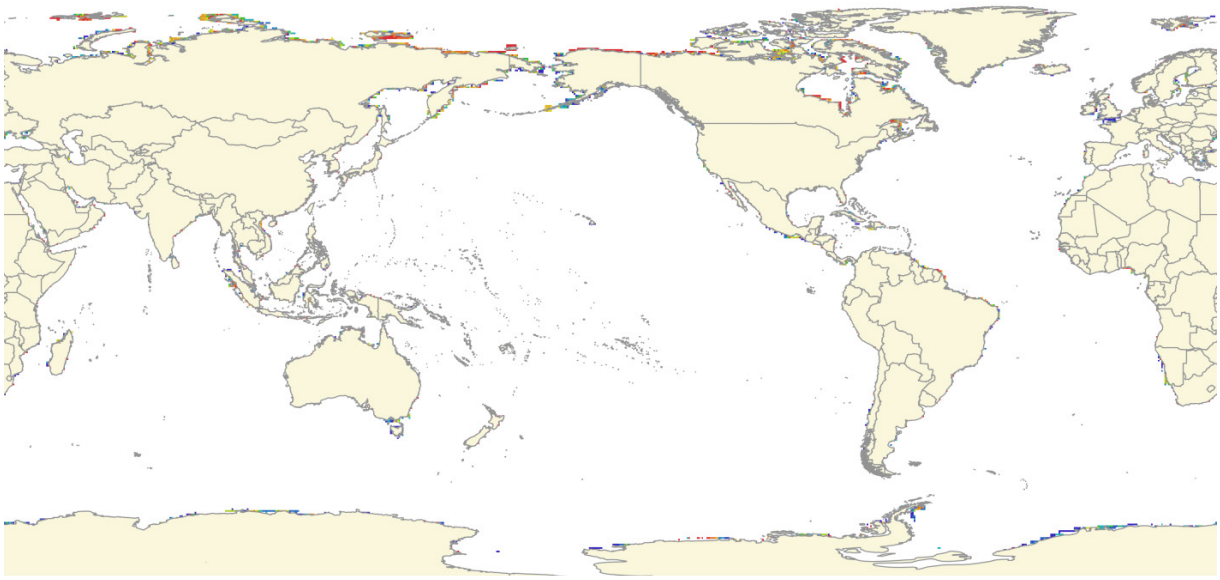

Figure 4.28. Frequency (number of years of occurrence per decade) of DHM Alert Level 2, 2040 (2040-2049), MM (RCP 4.5).

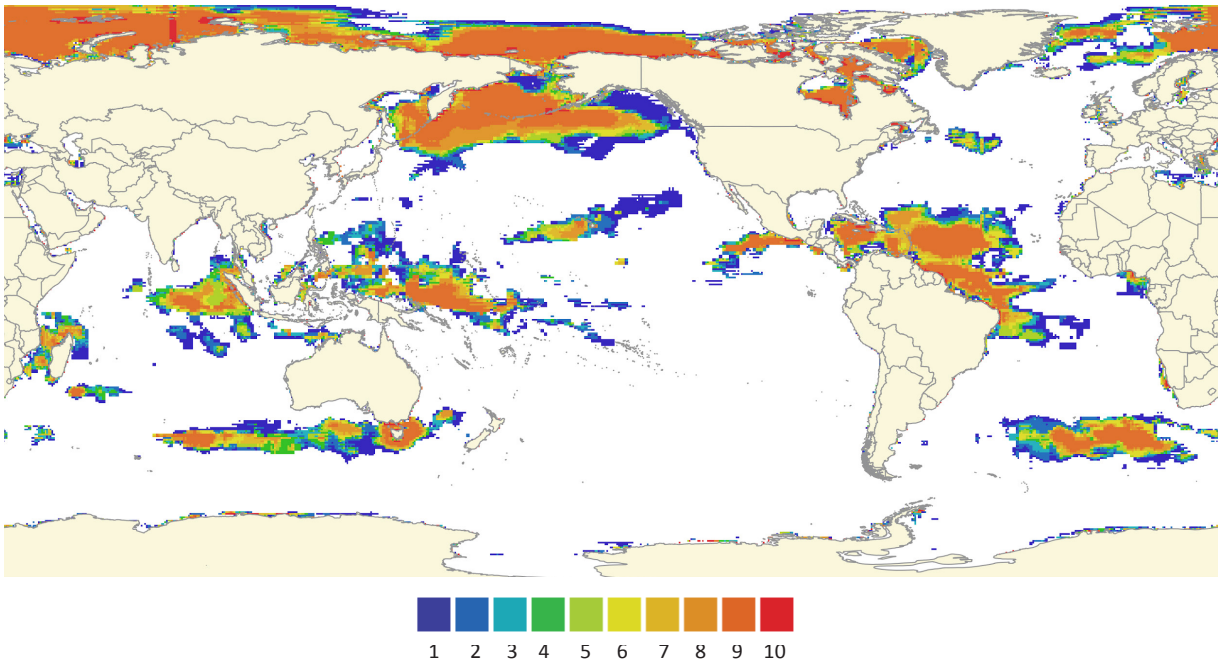

Figure 4.29. Frequency (number of years of occurrence per decade) of DHM Alert Level 2, 2050 (2050-2059), MM (RCP 4.5).

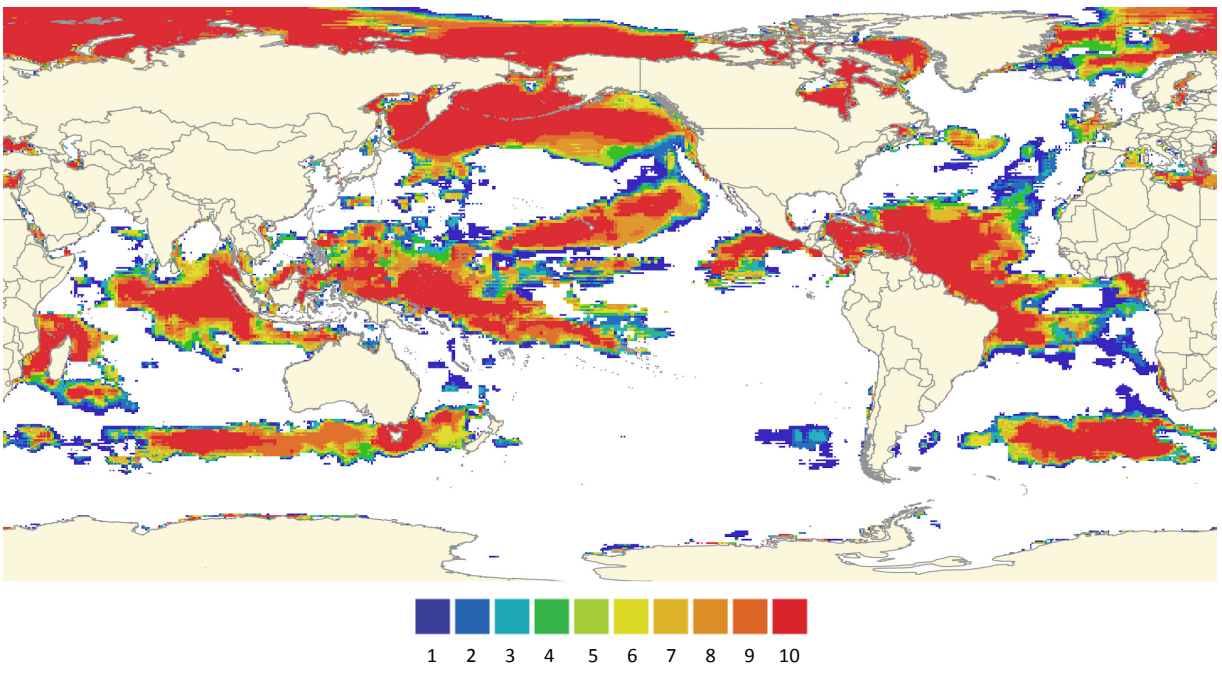

Decadal evolution of thermal stress under scenario BAU (RCP 8.5)

The evolution of the threat (demonstrated by the images below), comprises the projected frequency (number of yearly occurrence in a decade) of DHM Alert Level 2 for 2020 (Figure 4-30), 2030 (Figure 4-31), 2040 (Figure 4-32) and 2050 (Figure 4-33) under scenario BAU.

In the start of the time-series, a threat Level 2 occurs mostly in Northern Hemisphere latitudes, with some exception south of Tasmania, in the Pacific Ocean (East of Papua New Guinea and East of the Caribbean Sea). These initial locations with DHM Level 2 and a frequency between one to four per decade, significantly increased in frequency and extent throughout 2030s and 2040s. Decade 2050 shows that Alert Level 2 would occur each year in the decade, affecting virtually all seas except the Southern Ocean around the Antarctic.

Figure 4.30. Frequency (number of years of occurrence per decade) of DHM Alert Level 2, 2020 (2020-2029), BAU (RCP 8.5).

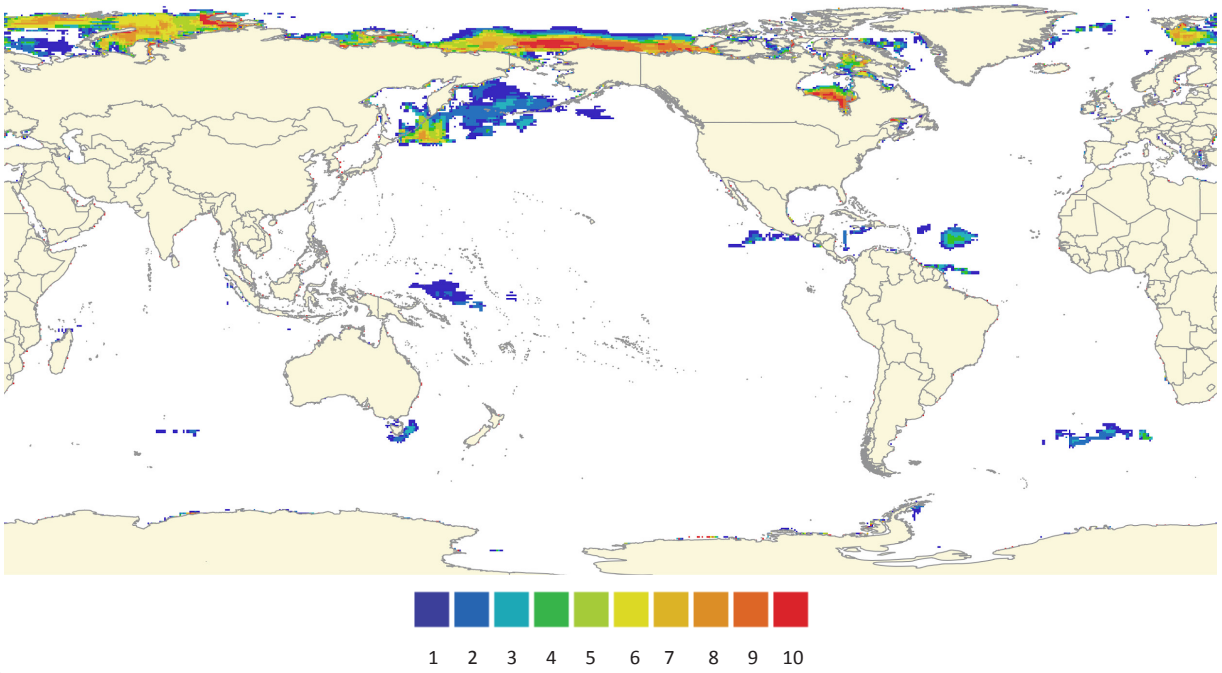

Figure 4.31. Frequency of DHM Alert Level 2, 2030 (2030-2039), BAU (RCP 8.5).

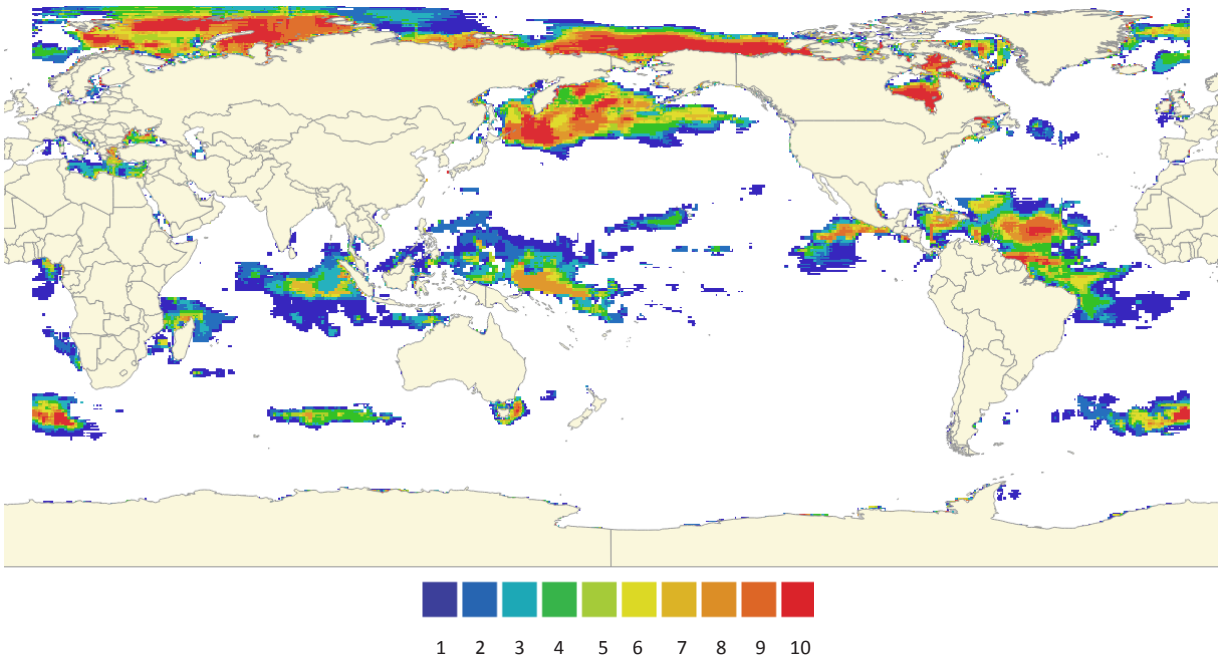

Figure 4.32. Frequency of DHM Alert Level 2, 2040 (2040-2049), BAU (RCP 8.5).

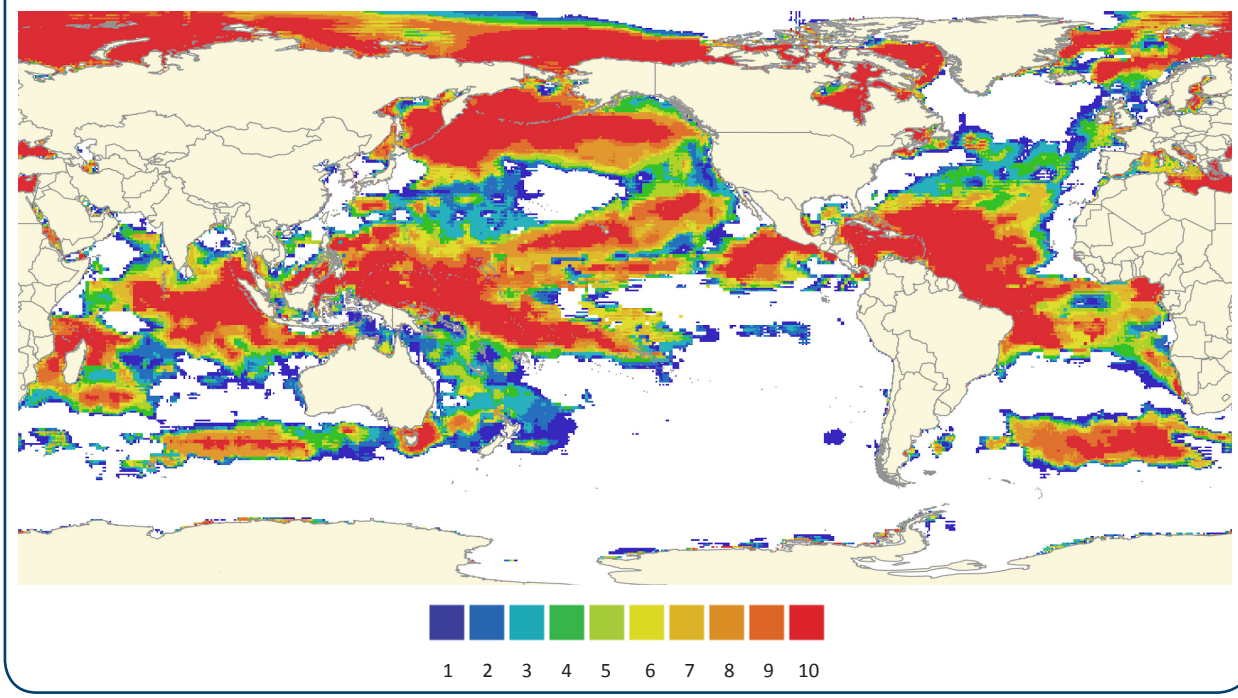

Figure 4.33. Frequency of DHM Alert Level 2, 2050 (2050-2059), BAU (RCP 8.5).

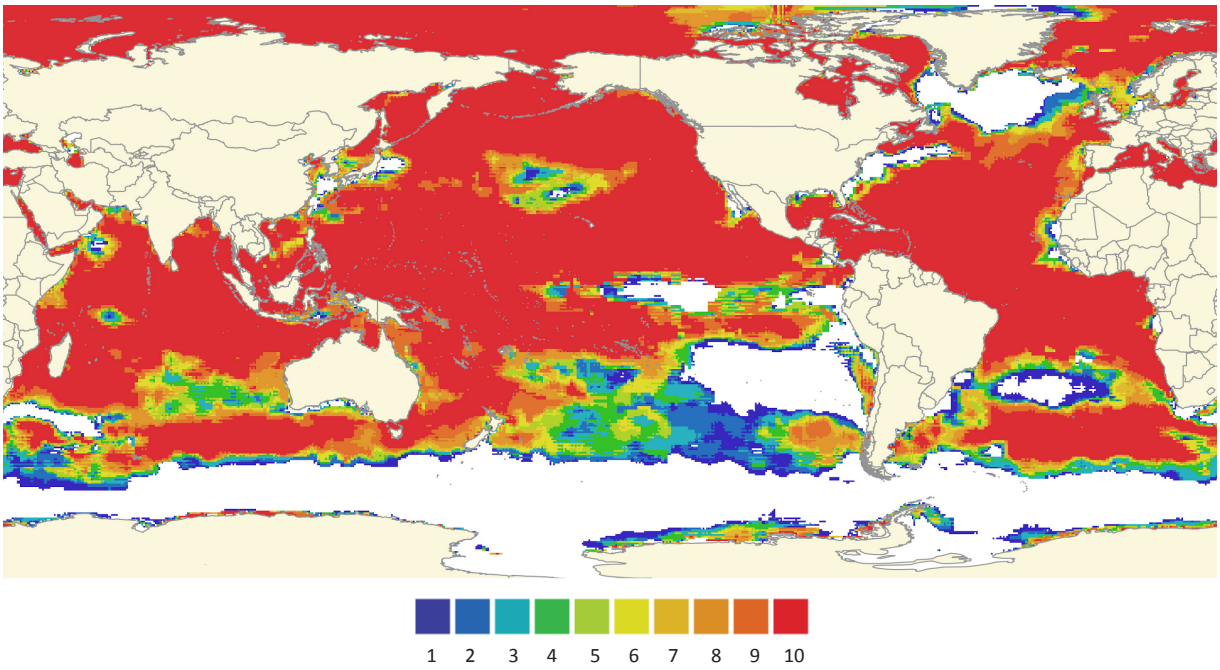

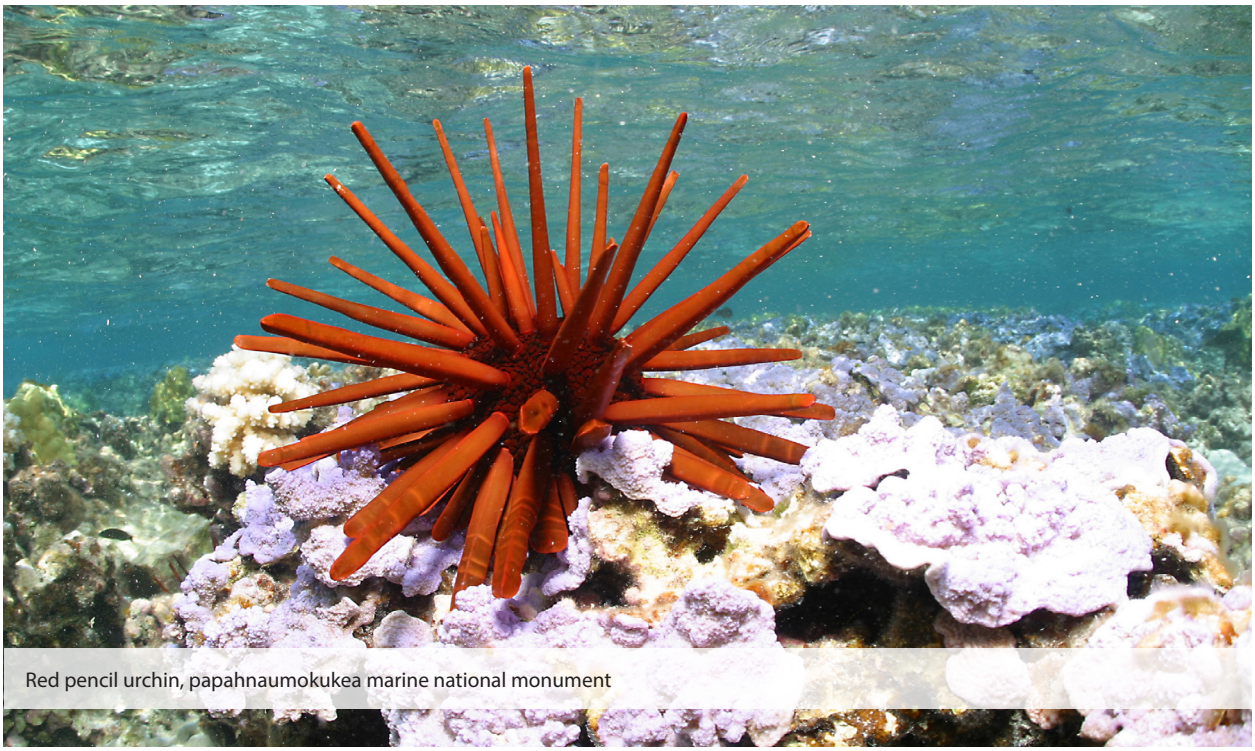

Red pencil urchin, papahnaumokukea marine national monument

References:

Cavalieri, D.J. and Parkinson, C.L. (2012). *Arctic sea ice variability and trends, 1979–2010.* The Cryosphere, 6, 881–889, www.the-cryosphere.net/6/881/2012/, doi:10.5194/tc-6-881-2012

Combal, B., 2014a, Time projections of Sea Surface Temperature, for RCP 4.5 and RCP 8.5, for decade 2020, 2030, 2040 and 2040, IOC-UNESCO, doi: 10.5281/zenodo.12781, https://zenodo.org/collection/user-ioc-code-cmip5

Combal, B., 2014b, Ensemble mean of CMIP5 TOS, for the period 1971 to 2000, IOC-UNESCO, doi:10.5281/zenodo.12843, https://zenodo.org/collection/user-ioc-code-cmip5

Combal, B, 2014c, Monthly climatology of CMIP5 models historical run, for 1971-2000, IOC-UNESCO, doi:10.5281/zenodo.12943, https://zenodo.org/collection/user-ioc-code-cmip5

Combal, B. and Caumont, H., 2016 (in press), Supporting marine sciences with Cloud services: technical feasibility and challenges, in *Cloud Computing in Ocean and Atmospheric Sciences ,* Vance, T.C., Merati, N., Yang, C, and M Yuan editors, Amsterdam, Elsevier.

Comiso, J.C. and Nishio, F. (2008). *Trends in the sea ice cover using enhanced and compatible AMSR-E, SSM/I, and SMMR data*, Journal of Geophysical Research: Oceans, vol. 113, C2, pp. 2156-2202, http://dx.doi.org/10.1029/2007JC004257, DOI:10.1029/2007JC004257

Donner S.D. (2009). Coping with Commitment: Projected Thermal Stress on Coral Reefs under Different Future Scenarios. PLoS ONE 4(6): e5712. doi:10.1371/journal.pone.0005712

Donner S.D., Heron S.F., Skirving W.J. (2008). *Future Scenarios: A Review of Modelling Efforts to Predict the Future of Coral Reefs in an Era of Climate Change*. In: van Oppen MJH, Lough JM, editors. Coral Bleaching: Patterns, Processes, Causes and Consequences. Berlin: Springer-Verlag. pp. 159–173.

Donner S.D., Skirving W.J., Little C.M., Hoegh-Guldberg O. and Oppenheimer M. (2005). *Global assessment of coral bleaching and required rates of adaptation under climate change*. Glob Change Biol 11: 2251–2265. doi: 10.1111/j.1365-2486.2005.01073.x.

Donner S.D., Knutson T.R. and Oppenheimer M. (2007). *Model-based assessment of the role of human-induced climate change in the 2005 Caribbean coral bleaching event*. Proc Natl Acad Sci U S A 104: 5483–5488. doi: 10.1073/pnas.0610122104

ESRL 2014, Long term SST climatology, http://www.esrl.noaa.gov/psd/data/gridded/data.noaa.oisst.v2.html, (accessed February 2014)

IPCC, 2013: Climate Change 2013: The Physical Science Basis. Contribution of Working Group I to the Fifth Assessment Report of the Intergovernmental Panel on Climate Change Stocker, T.F., Qin D., Plattner G.-K., Tignor M., Allen S.K., Boschung J., Nauels A., Xia Y., Bex V. and Midgley P.M. (eds.). Cambridge University Press, 1535 pp.

Lennon, Erika. 2008, A Tale of Two Poles: A Comparative Look at the Legal Regimes in the Arctic and the Antarctic, Sustainable Development Law and Policy, pp. 32-36, vol. 65-66.

Lin, X., and Johnson R.H. (1996). Kinematic and thermodynamic characteristics of the flow over the western Pacific warm pool during TOGA COARE. J. Atmos. Sci., 53, 695–715.

Long term climatology: sst.ltm.1971-2000, http://www.esrl.noaa.gov/psd/data/gridded/data.noaa.oisst.v2.html

Monthly SST, for estimating variance, 1981-2000, ftp://ftp.emc.ncep.noaa.gov/cmb/sst/oimonth_v2/

Mehta, V.M. and Mehta, A.V, *Natural decadal-multidecadal variability of the Indo-Pacific Warm Pool and its impacts on global climate*. The Centre for Research on the Changing Earth System (CRCES). http://www.crces.org/presentations/dmv_ipwp/ (accessed July 2014)

Meier W.N, Stroeve, J., Barrett, A. and Fetterer, F. (2012). A simple approach to providing a more consistent Arctic sea ice extent time series from the 1950s to present, Cryosphere, 6, 1359-1368

Oldenborgh, G.J, Doblas Reyes, F.J., Drijfhout, S.S. and Hawkins E. (2013). *Reliability of regional climate model trends*. Environmental Research Letters, Vol. 8, N. 1, doi:10.1088/1748-9326/8/1/014055, http://iopscience.iop.org/1748-9326/8/1/014055/

Programme for Climate Model Diagnosis and Intercomparison, http://www-pcmdi.llnl.gov/about/index.php, accessed on 19 November 2014

Reynolds, R.W., Rayner, N.A., Smith, T.M., Stokes, D.C. and Wang, W. (2002). *An improved in situ and satellite SST analysis for climate*. J. Climate, 15, 1609-1625.

Taylor, K.E, Stouffer, R.J. and Meehl, G.A. (2011). *A Summary of the CMIP5 Experiment Design*, http://cmip-pcmdi.llnl.gov/cmip5/docs/Taylor_CMIP5_design.pdf, http://cmip-pcmdi.llnl.gov/cmip5/experiment_design.html (accessed October 2014)

Taylor, K. E., Stouffer, R. J. and Meehl, G. A (2012). *An overview of CMIP5 and the experimental design*. Bull. Am. Meteorol. Soc. 93, 485–498, DOI: 10.1175/BAMS-D-11-00094.1

Wang H. and Mehta, V.M. (2008). Decadal variability of the indo-pacific warm pool and its association with atmospheric and oceanic variability in the ncep–ncar and soda reanalyses, J. Climate, 21, 5545–5565, doi: http://dx.doi.org/10.1175/2008JCLI2049.1

Webster, P. J. (1994). The role of hydrological processes in ocean-atmosphere interaction. Rev. Geophys., 32, 427–476

World Climate Research Programme, WCRP Working Group on Coupled Modeling, http://www.wcrp-climate.org/wgcm, accessed on 19 November 2014

Wyrtki, K. (1989) *Some thoughts about the West Pacific Warm Pool. Proc. Western Pacific Int. Meeting and Workshop on TOGA/COARE*. Noumea, New Caledonia, 99–109. [Available from Centre ORSTOM de Noumea, B.P. A5 98848, Noumea Cedex, New Caledonia.]

Xiao-Han Y., Chung-Ru, H., Quanan, Z. and Klemas, V. (1992). *Temperature and Size Variabilities of the Western Pacific Warm Pool*, Science, Vol. 258, pp. 1643-1645

Xie, F., Li J., Tian, W., Li, Y. and Feng, J. (2014). Indo-Pacific Warm Pool Area Expansion, Modoki Activity, and Tropical Cold-Point Tropopause Temperature Variations, Sci. Rep., 4:4552

Yan Xue, NOAA_OI_SST_V2 data provided by the NOAA/OAR/ESRL PSD, Boulder, Colorado, USA, from their Web site at http://www.esrl.noaa.gov/psd/